International Journal of Engineering

Journal Homepage: www.ije.ir

Computational Study of Excitation Controlling Parameters Effect on Uniform Beam Deformation under Vibration

P. Lap-Arparat, K. Tuchinda*

Material Manufacturing and Surface Engineering Research Center (MaSE),The Sirindhron International Thai-German Graduate School of Engineering (TGGS), King Mongkut's University of Technology North Bangkok (KMUTNB), Bangkok, Thailand

P A P E R I N F O

Paper history:
Received 13 August 2022
Received in revised form 30 August 2022
Accepted 18 September 2022

Keywords:
Mode Shape Analysis
Geometry Ratio
Structural Response
Shape Deformation
Transverse Vibration
Uniform Beam

A B S T R A C T

Understanding a structure's behavior is necessary for most applications, especially excitation in ultrasonic applications. Currently, ultrasonic devices are used in various fields and have an essential role in nondestructive testing (NDT). The structure's behavior must be concerned with achieving the best practice. The structural vibrational behavior depends on natural frequency and mode shape. This study attempted to determine the effect of influence parameters on shape deformation for designing the adequate excitation condition. In this study, the influence parameters of a uniform beam, including geometry, support condition, and material, were included to investigate their effect on the frequency, mode shape, and structural response. The result showed the significant influence of a structure's length and support condition on the mode frequency, dramatically decreasing mode frequency for extended installation and cantilever support. This study investigated the three common mode shapes revealed that the longitudinal bending shape dominated due to the loading direction. Therefore, the shape deformation of the structure is mainly governed by the external excitation source, and the high structural response is received by applying the excitation near the antinode position of the vibration. Nevertheless, the computational result showed a good agreement with the analytical validation with less than 1 % error. The study leads to understanding the vibration, which can be further used for either the effective sensor attachment or designing the vibration control of ultrasonic applications.

***doi**: 10.5829/ije.2023.36.01a.08*

1. INTRODUCTION

Recently, shape deformation due to vibration has been a concern in various contexts, especially structural analysis [1, 2]. A structure's natural frequency (ω_n) is important in structural vibration, showing a less damping force effect [3]. The geometry and material of the structure influence the natural frequency [4-6]. Moreover, the support type also affects the natural frequency. In most cases, the natural frequency is cognizant for a structural study due to the mechanical resonance. The resonant frequency is the frequency of external force that matches the structure's natural frequency and causes a great amplitude of the vibration [7]. Since the incident of Tacoma Narrows Bridge in 1940, when the bridge collapsed due to resonance generated by the wind. The wind speed was 68 km/h and frequency of 0.2 Hz, nearly close to the bridge's natural frequency (approximately 1 Hz), initiated the vibration of the bridge together with the aeroelastic fluttering. This caused the bridge to oscillate periodically with increasing amplitude in the torsional mode, where the two halves of the bridge twisted in opposite directions before collapsing [8, 9]. The natural frequency and vibrational mode shape of a structure are prime concerns to prevent a recurrence of a similar situation.

Therefore, the vibration study is essential to understand the behavior of the structure. The influence parameters have been investigated for their effect on the vibration. Regarding another researcher's works, many related variables such as boundary conditions [10, 11], stiffness [12], and shape [13] were either experimentally or analytically investigated for their effect on the

*Corresponding Author Institutional Email: karuna.t@tggs.kmutnb.ac.th (K. Tuchinda)

Please cite this article as: P. Lap-Arparat, K. Tuchinda, Computational Study of Excitation Controlling Parameters Effect on Uniform Beam Deformation under Vibration, ***International Journal of Engineering, Transactions A: Basics***, Vol. 36, No. 01, (2023), 60-70

deformation under the vibration. Nevertheless, as reported, those variables influenced the deformation, which should be considered in the vibrational study. Furthermore, some variables were applied to the safety design of the vibration control [14] and structural construction [15-17].

The natural frequency and vibrational mode understanding is currently applied differently for varying applications such as tuning folk and ultrasonic transducer [18, 19]. The design of vibrating devices that are required to operate at resonance to optimize the vibrational amplitude; an example is an ultrasonic transducer. An ultrasonic transducer is a device that converts an electrical signal into a vibration via piezoelectric disks located in between the coupled materials. Generally, the coupled materials have a natural frequency similar to the vibration of the piezoelectric disk; this causes the highest amplitude at the vibrating tip. Furthermore, the mode shape of the vibration is correspondingly designed to perform shape deformation as a targeting purpose, making it operate at a fixed frequency [19]. Nowadays, ultrasonic devices are used in various fields, including medical and industrial [20-22]. Ultrasonic devices have an important role in nondestructive testing (NDT), whether ultrasonic testing or vibrothermography. However, excitation at resonance frequency can cause damage to structures or systems due to the large deformation. Conversely, it can enhance the power of a low-power excitation device.

According to Xu et al. [23], a low-power ultrasonic transducer (5-14 W) was used to apply the excitation for vibrothermography crack detection. The artificial surface crack was created on a thin beam and clamped on both ends. Under the excitation, the known crack was hardly detected since the power was much lower than the literature, which is up to 2 kW [24]. Although, adjusting the excitation position can improve the detection, which provides a clearer indication of the crack. Consequently, applying an excitation or sensor attachment requires understanding the structural behavior and mode shape to optimize the expected result.

In this study, the structural behavior of the objects was simulated at various frequencies to provide an understanding and the effect of the influenced parameters on a vibrational mode shape. The object's geometry and material were varied, including the support types to provide different degrees of freedom (DOF). The study attempted to understand vibrational behavior to design the effective conditions for excitation based on a laboratory scale of uniform beam excitation. Moreover, steady-state dynamic analysis was applied to investigate each condition's frequency response and structural behavior. The overall research methodology flow is presented as illustrated in Figure 1. This work is the 1st attempt to understand the effect of the geometry ratio including the material and support conditions on vibrational characteristics aiming to develop a computational framework to be used in the design of the excitation controlling system for vibration-based NDT.

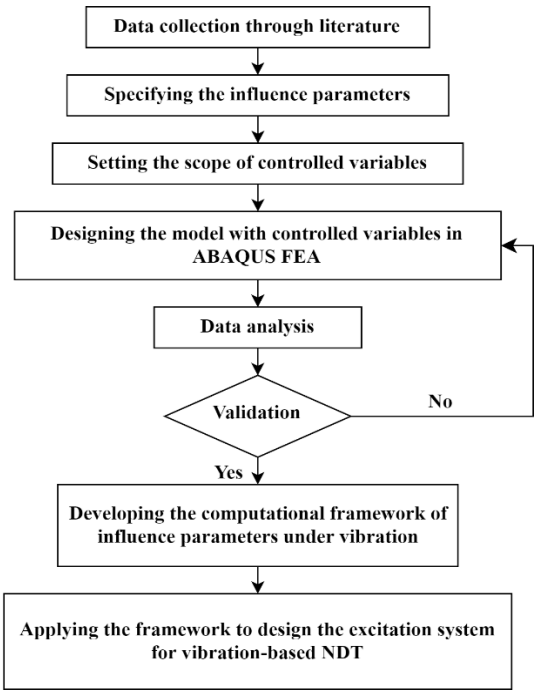

Figure 1. Flowchart of the study

2. PROCEDURE

2. 1. Simulation Model Setup The study of shape deformation and structural behavior was simulated in ABAQUS FEA. In the simulation, a 3-Dimensional model of a rounded rectangular rod was created, as shown in Figure 2. The rectangular rod structure was selected for the study as it is one of the most common structures used for engineering applications. The aspect ratio was applied to differentiate the structure's geometry which has controlled the shape of the structure, as detailed in Table 1. The non-dimensional height of the structure was initially assigned as 10. The scope of the geometry ratio was based on the range of engineering parts used in the industrial automation system which is the main interest of the current work. According to the predefined aspect ratio, 27 models were created and studied under different conditions based on the vibration analysis of a uniform beam. The support conditions were also varied: fixed ends and a cantilever. Moreover, two different metallic materials, i.e., steel and aluminum, were included in the study, and their properties are summarized in Table 2. In total, 108 cases were studied. The 8-node hexahedral elements with reduced integration (C3D8R) were globally applied to optimize the computational time of the simulation model. The work

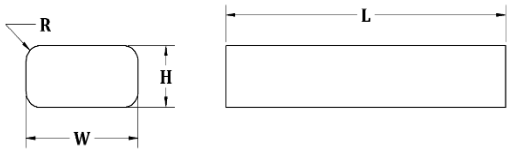

Figure 2. Model shape and dimension

aimed to develop a computational framework to be used in the design of the excitation controlling system for vibration-based NDT from the vibrational characteristic under different conditions of vibration.

2. 2. Mode Shape Analysis Frequency analysis of the linear perturbation was applied to investigate the vibrational mode shape of the structure. The effect of the geometry above, including the boundary conditions, on each mode's vibrational frequency, was observed, detailed in section 3. Moreover, the shape and the behavior of deformation were also investigated.

2. 3. Steady-state Dynamic Analysis The behavior of the structure under the vibration was studied in the steady-state dynamic modal. A 10 N of harmonic load (P) was applied at different locations of x to investigate the structural behavior, as illustrated in Figure 3.

3. RESULTS AND DISCUSSION

The first five modes are taken to show the behavior of the vibration. Three common shapes were included in the first five modes, which were (1) Longitudinal bending, (2) Lateral bending, and (3) Torsional bending (Twist), as shown in Figure 4. The higher order of the mode shape which occurred at higher vibrational frequency provides a more significant number for the antinode vibration, an example of the node and antinode in the structural vibration is illustrated in Figure 5. The effect of the conditions above on mode shape was shown by plotting the vibrational frequency of each mode, as can be seen in Figure 6. From the comparison, the major effect of vibrational frequency was revealed on the length of the structure and the type of support condition. The greater the length significantly decreased the vibrational frequency of each mode, in the same manner as the cantilever support significantly diminished the frequency compared with the fixed ends support. For the corner radius, a minor effect appeared as the larger radius was slightly decreased at the mode shape frequency. Furthermore, the ratio of width to height (W/H) had a complex impact on the frequency, which displayed a noticeable difference in some modes.

However, the ratio dominated the shape deformation; the higher ratio revealed more of the longitudinal bending shape in the first five modes.

TABLE 1. Geometry ratio

R/H	W/H	L/H
0	1	10
0.25	2	50
0.5	5	100

TABLE 2. Material property

Material	Density (kg/m^3) [14]	Elastic modulus (GPa) [14]	Poisson's ratio [15]
Steel	7900	200	0.28
Aluminum	2700	70	0.33

Moreover, the ratio of W/H = 1 has a similar frequency between mode 1 and mode 2 likewise in mode 3 and mode 4. However, the deformation shapes were different, i.e. bending in different directions, as shown in Figure 7. Considering the structure's material, there seemed to be no effect on the vibrational frequency and shape deformation. Lastly, the shapes of each mode are listed in Table 3

Note: the shapes are listed in the following format

X#Y

where X = Bending shape;

B: Longitudinal, LB: Lateral,TB: Torsional

Y = Number of antinodes

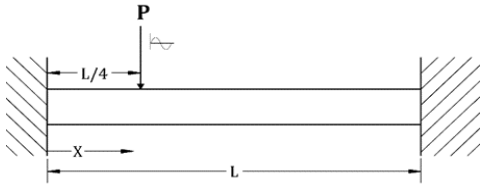

(a) Fixed ends support

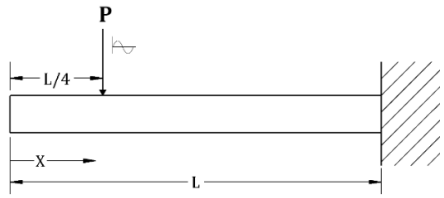

(b) Cantilever support

Figure 3. Example model of harmonic load at x = L/4 in steady-state dynamic analysis

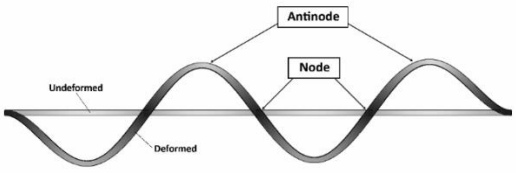

Figure 5. Nodes and antinodes of structural vibration

(a) Longitudinal bending (b) Lateral bending (c) Torsional bending

Figure 4. Bending shape

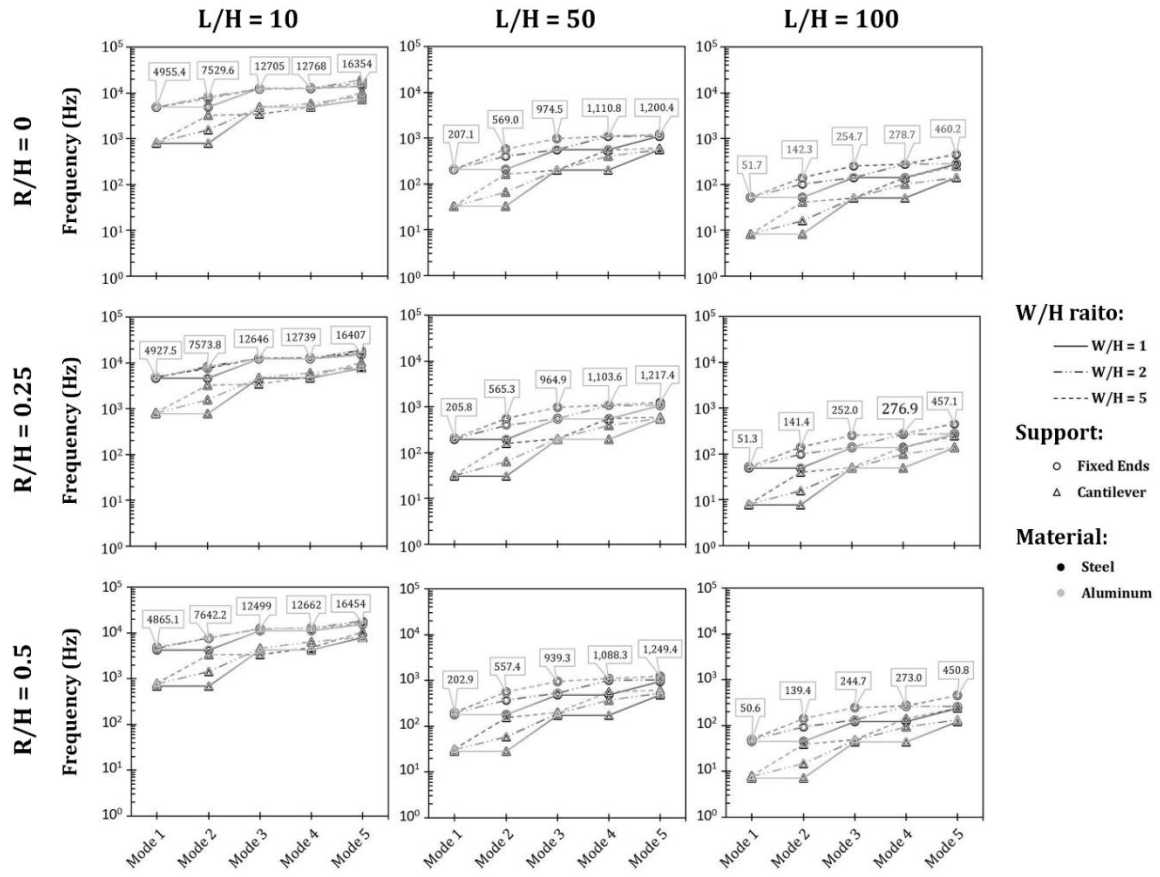

Figure 6. The effect of geometry on the vibrational frequency

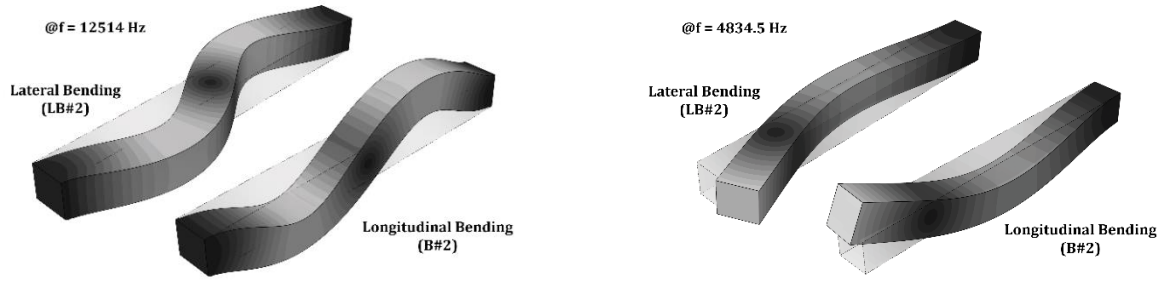

(a) Fixed ends support (b) Cantilever support

Figure 7. Example of shape deformation of the geometry ratio W/H = 1 at a similar frequency

TABLE 3. List of shape deformation with several antinodes

Support:		Fixed ends					Cantilever				
R/H = 0											
W/H	**L/H**	**Mode**									
		1	**2**	**3**	**4**	**5**	**1**	**2**	**3**	**4**	**5**
	10	LB#1	B#1	LB#2	B#2	TB	B#1	LB#1	LB#2	B#2	TB
1	50	B#1	LB#1	B#2	LB#2	B#3	B#1	LB#1	B#2	LB#2	B#3
	100	B#1	LB#1	B#2	LB#2	B#3	B#1	LB#1	B#2	LB#2	B#3
	10	B#1	LB#1	TB	B#2	LB#2	B#1	LB#1	B#2	TB	LB#2
2	50	B#1	LB#1	B#2	B#3	LB#2	B#1	LB#1	B#2	LB#2	B#3
	100	B#1	LB#1	B#2	B#3	LB#2	B#1	LB#1	B#2	LB#2	B#3
	10	B#1	TB	B#2	LB#1	TB	B#1	TB	LB#1	B#2	TB
5	50	B#1	B#2	LB#1	B#3	TB	B#1	LB#1	B#2	B#3	TB
	100	B#1	B#2	LB#1	B#3	B#4	B#1	LB#1	B#2	B#3	LB#2
R/H = 0.25											
W/H	**L/H**	**Mode**									
		1	**2**	**3**	**4**	**5**	**1**	**2**	**3**	**4**	**5**
	10	LB#1	B#1	LB#2	B#2	TB	LB#1	B#1	LB#2	B#2	TB
1	50	LB#1	B#1	LB#2	B#2	LB#3	LB#1	B#1	LB#2	B#2	LB#3
	100	LB#1	B#1	LB#2	B#2	LB#3	LB#1	B#1	LB#2	B#2	LB#3
	10	B#1	LB#1	B#2	TB	LB#2	B#1	LB#1	B#2	TB	LB#2
2	50	B#1	LB#1	B#2	B#3	LB#2	B#1	LB#1	B#2	LB#2	B#3
	100	B#1	LB#1	B#2	B#3	LB#2	B#1	LB#1	B#2	LB#2	B#3
	10	B#1	TB	B#2	LB#1	TB	B#1	TB	LB#1	B#2	TB
5	50	B#1	B#2	LB#1	B#3	TB	B#1	LB#1	B#2	B#3	TB
	100	B#1	B#2	LB#1	B#3	B#4	B#1	LB#1	B#2	B#3	LB#2
R/H = 0.5											
W/H	**L/H**	**Mode**									
		1	**2**	**3**	**4**	**5**	**1**	**2**	**3**	**4**	**5**
	10	LB#1	B#1	LB#2	B#2	TB	LB#1	B#1	LB#2	B#2	TB
1	50	LB#1	B#1	LB#2	B#2	LB#3	LB#1	B#1	LB#2	B#2	LB#3
	100	LB#1	B#1	LB#2	B#2	LB#3	LB#1	B#1	LB#2	B#2	LB#3
	10	B#1	LB#1	B#2	TB	LB#2	B#1	LB#1	B#2	TB	LB#2
2	50	B#1	LB#1	B#2	LB#2	B#3	B#1	LB#1	B#2	LB#2	B#3
	100	B#1	LB#1	B#2	LB#2	B#3	B#1	LB#1	B#2	LB#2	B#3
	10	B#1	TB	B#2	LB#1	TB	B#1	TB	LB#1	B#2	TB
5	50	B#1	B#2	LB#1	B#3	TB	B#1	LB#1	B#2	B#3	TB
	100	B#1	B#2	LB#1	B#3	B#4	B#1	LB#1	B#2	B#3	LB#2

The steady-state dynamic analysis described the structural response by a log-log scale plot between the normalized deformation magnitude and frequency. Firstly, the structural response under the harmonic loading at L/2 was observed for the response along the length of the structure. A sharp corner square rod (R/H =

0, W/H = 1) with fixed ends support condition was selected in this investigation. The deformation magnitude ratio (minimum/maximum) along the length was plotted as shown in Figure 8.

Figure 8 informs the response from different locations of x/L under the harmonic loading. The behavior of the responses corresponded with the mode shape, which was noticeably increased at the frequency of the mode shape. The longitudinal bending type only occurred in this investigation. The magnitudes of deformation along the lengths were different. However, the behavior was similar for all locations of x/L, which increased while approaching the mode frequencies, except for x/L equal to 0 and 1, which had no responses under loading due to the support condition. To understand the behavior of the structure response, the response at x/L = 0.5 at the different locations of the harmonic load was plotted as shown in Figure 9.

Figure 9 shows the different responses seen in L/H = 10 and 100. Mode 3 was more responsive to the loading at L/4 rather than L/2. Considering shape deformation, modes 1, 3, and 5 showed the longitudinal bending shape, which has a different number of antinodes. The deformation shape of the third mode revealed 2 antinodes on the vibration, as shown in Figure 10. According to the loading location, L/4 was located close to the antinode, and L/2 was located close to the node of this vibrational mode. Therefore, the loading at L/4 provided a higher response in mode 3, as shown in Figure 9.

Considering the aspect ratio of the geometry, the response under the harmonic loading at L/4 with fixed ends support was plotted on a stacked log-log chart for a clear display of the geometry effect. The behavior of deformation magnitude at x/L = 0.5 was only concerned in the comparison. The effect of the geometry ratio is shown in Figure 11. Furthermore, the effect of the support-type and structural material was included, as can be seen in Figures 12 and 13, respectively, which were investigated on a sharp corner square rod. Figure 11 shows the difference in the behavior of the structural response from the different geometry. The longitudinal bending only appeared under vibration for the sharp square rod (R/H = 0, W/H = 1). Moreover, the higher ratio of R/H and W/H revealed a higher chance of lateral and torsional bending. However, longitudinal bending mainly occurred due to the direction of loading. The

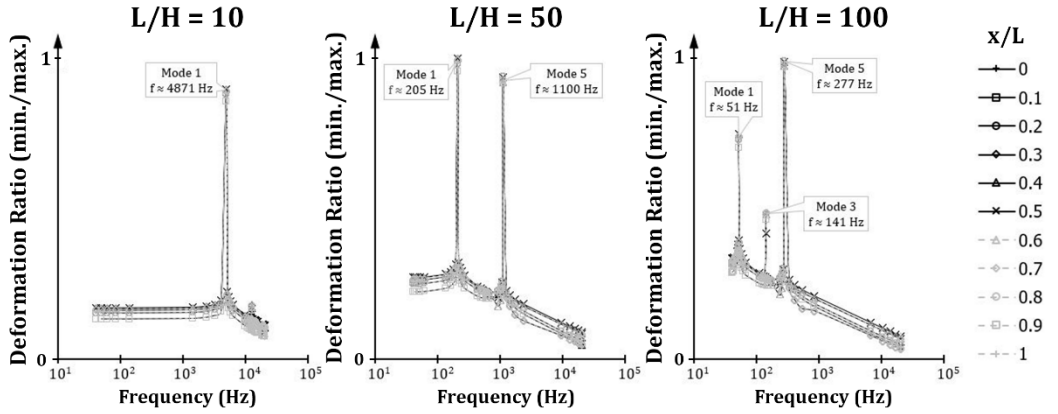

Figure 8. The structural response of the different locations of x/L

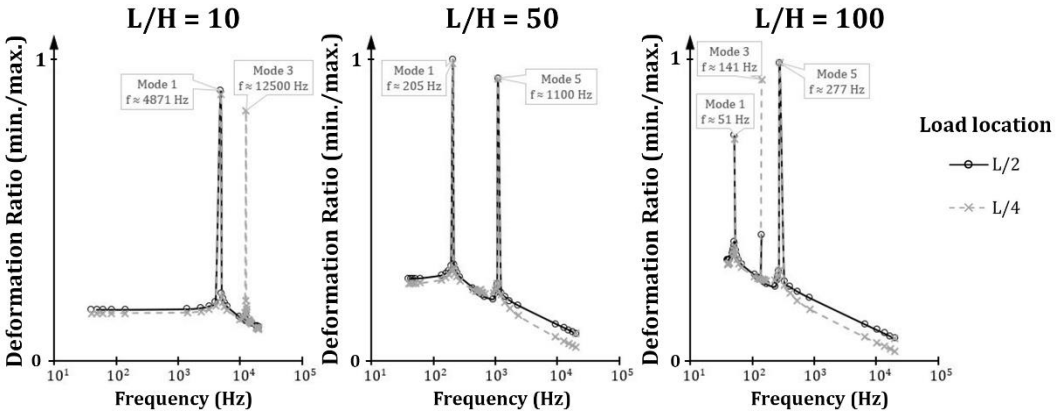

Figure 9. The effect of different loading locations on the structural response

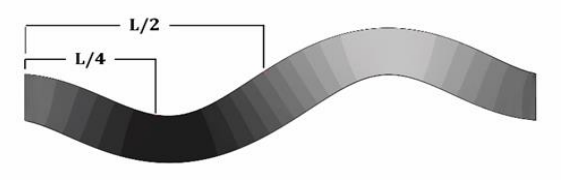

Figure 10. The third mode of sharp corner square rod

cantilever condition for the support condition revealed the torsional bending in the length ratio L/H =10; the rest were longitudinal bending. In contrast, the condition of the fixed ends only revealed longitudinal bending. Furthermore, the effect of structural material in Figure 13. shows a similar trend and shape of the response. In terms of deformation magnitude, a more extended structure had a higher magnitude of deformation, and the mode of longitudinal bending shape was dominant, with the highest response among the deformation shapes. Lastly, aluminum material has a higher response than steel.

The computational results were compared with similar studies, either experimental or computational. The natural frequency and the structure's response under the vibration could not be compared directly due to the difference in structural geometry. Nonetheless, the small difference in the natural frequency of steel and aluminum was verified in the experimental study of Young et al [25]. Moreover, the shape deformation under transverse vibration of the second structural mode was compared with another experimental study by Hassanpour et al. [26]. Figure 14 shows the shape deformation of a uniform beam with fixed ends. The obtained experimental data roughly provided the shape deformation since only seven measuring points were used in their study. However, the shape deformation along the length had a similar trend. In addition, similar studies correspond well with the current work [27]. In short, the investigation of multi-shape uniform beam revealed the characteristic of the natural frequency at each mode of the structure which was uniquely dependent on boundary conditions and geometry. Under the excitation, the structure vibrated in the direction of the excitation, which governed the shape deformation, i.e., the longitudinal bending occurred from vertical excitation (transverse vibration).

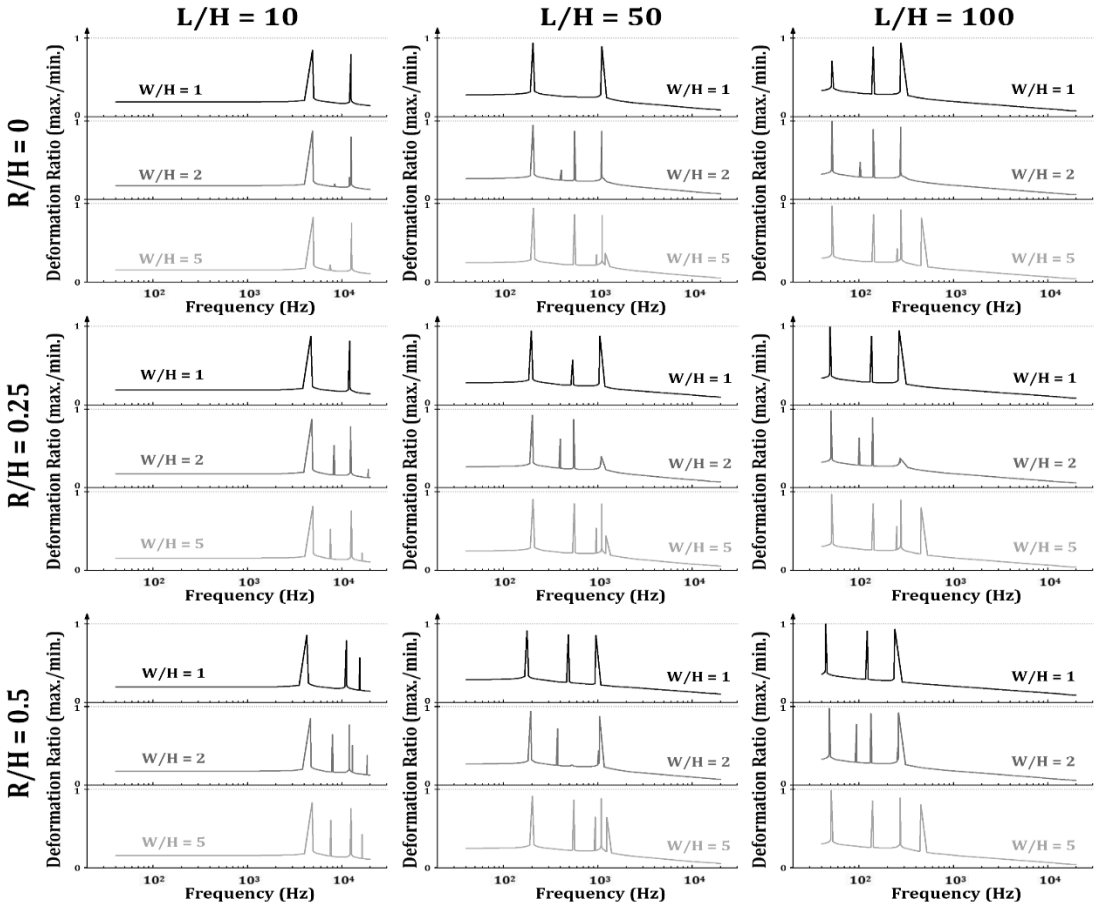

Figure 11. The effect of geometry ratio on the structural response

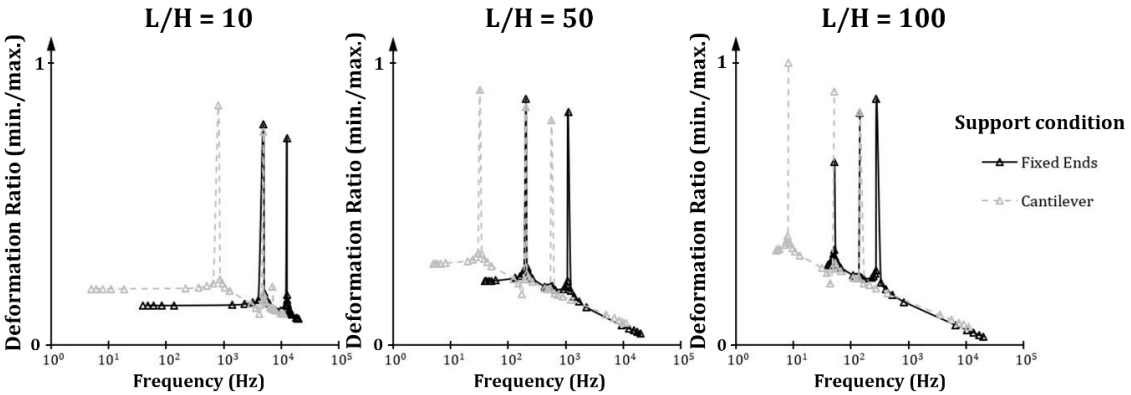

Figure 12. The effect of support conditions on the structural response

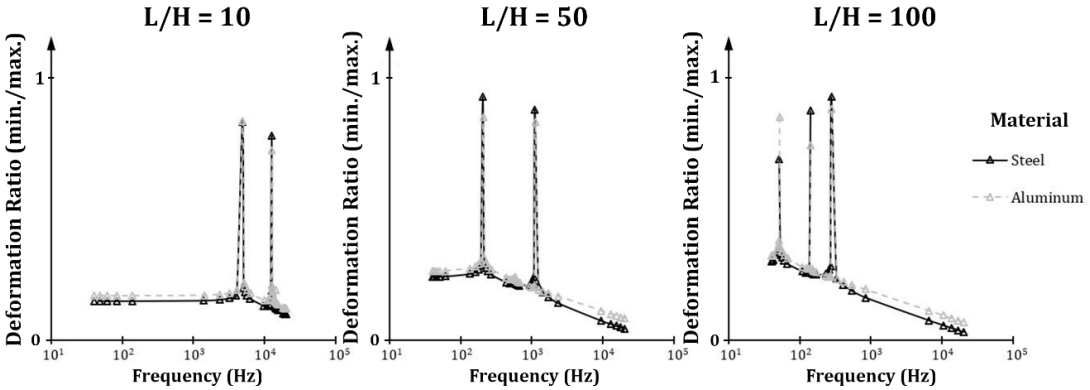

Figure 13. The effect of material on the structural response

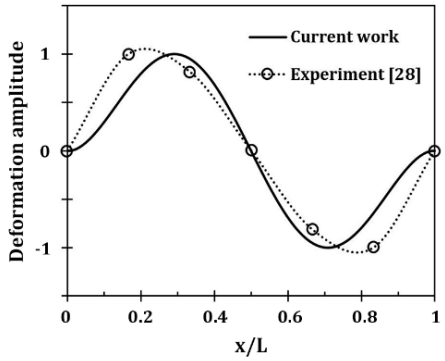

Figure 14. The second mode of the uniform rectangular beam with fixed ends under transverse vibration

Regarding the vibrational mode, the mode of vibration depends on the position and frequency of the excitation. The excitation at the antinode of vibration with a similar mode frequency as the structure would control the occurrence mode of vibration. Nevertheless, the excitation at natural frequency was not recommended for high-power excitation devices, which can cause a failure due to large deformation.

4. ANALYTICAL VALIDATION

According to theoretical calculation, the natural frequency of the uniform beam with both ends fixed can be calculated via the following expression [25, 28]:

$$\omega_n = \frac{K_n}{2\pi}\sqrt{\frac{EI}{\rho AL^4}} \quad (1)$$

where, ω_n = Natural frequency (Hz)
E = Elastic modulus (Pa)
I = Area moment of inertia (m^4)
ρ = Density (kg/m^3)
A = Cross-sectional area (m2)
L = Length (m)
K_n = Mode constant

Equation (1) was used to validate the FEM results of the sharp corner (R/H = 0) structure with L/H = 100, as detailed in Table 4. The validation was performed on the mode frequency of the longitudinal bending shape under the transverse vibration. The comparison showed a good agreement with an error of less than 1 %.

Moreover, the mode shape (Longitudinal bending) of a uniform beam under the transverse vibration with both

ends fixed conditions was governed by the following equation [29, 30].

$$W_n(x) = C_n\left[\left(\sinh\beta_x x - \sin\beta_n x\right) + \mu\left(\cosh\beta_n x - \cos\beta_n x\right)\right]$$
$$\mu = \frac{\sinh\beta_n l - \sin\beta_n l}{\cos\beta_n l - \cos h\beta_n l} \quad (2)$$

where $\beta_n l$ is the mode parameter which is listed in Table 5 and C_n is the magnitude constant of vibration. From Equation (2), the nodal position of the vibration is shown in Table 5. To validate the FEM results, four mode shapes of the structural ratio R/H =0, W/H = 5, and L/H = 100 were plotted, as shown in Figure 15, to compare the position of the node with the analytical data. The nodal positions of the FEM result were almost identical to the theoretical calculation, which confirmed the correctness of the simulation. Since the behavior of the structural response is governed by natural frequency and mode shape. Consequently, the aforementioned steady-state analysis is undoubtedly certified.

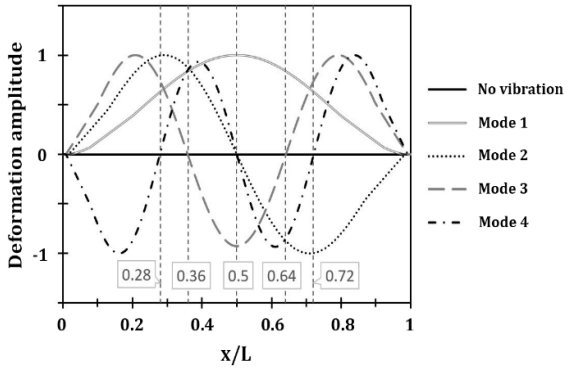

Figure 15. Longitudinal mode shape under the transverse vibration of the FEM method

TABLE 4. Comparison of the natural frequency for the longitudinal bending mode

W/H = 1				
Mode	K_n **[25]**	$\omega_{n,\ Analytic}$ **(Hz)**	$\omega_{n,FEM}$ **(Hz)**	**Error (%)**
1	22.4	51.808	51.470	0.653
2	61.7	142.704	141.760	0.662
3	121	279.857	277.570	0.817
W/H = 1				
Mode	K_n **[25]**	$\omega_{n,\ Analytic}$ **(Hz)**	$\omega_{n,FEM}$ **(Hz)**	**Error (%)**
1	22.4	51.808	51.509	0.578
2	61.7	142.704	141.860	0.591
3	121	279.857	277.790	0.739
W/H = 1				
Mode	K_n **[25]**	$\omega_{n,\ Analytic}$ **(Hz)**	$\omega_{n,FEM}$ **(Hz)**	**Error** (%)
1	22.4	51.808	51.670	0.267
2	61.7	142.704	142.310	0.276
3	121	279.857	278.700	0.414
4	200	462.574	460.170	0.520

TABLE 5. Mode parameters ($\beta_n l$) and nodal position of fixed-fixed uniform beam

Mode	$\beta_n l$ **[29]**	**Nodal position/L [25, 31]**
1	4.7300	0.0, 1.00
2	7.8532	0.0, 0.50, 1.00
3	10.9956	0.0, 0.33, 0.67, 1.00
4	14.1372	0.0, 0.25, 0.50, 0.75, 1.00

5. CONCLUSION

In this study, the influence parameters including geometry, support condition, and material are investigated for their effect on the natural frequency, mode shape, and structural response. Regarding geometry ratio, the structural length had a major effect on the mode frequency of vibration. A more extended structure had a lower natural frequency, and the corner radius of the structure rarely affected the frequency. The width of the structure was dominated by the mode shape, which had a more torsional effect on a larger width. Furthermore, the cantilever support significantly decreased the frequency compared to fixed-fixed conditions, and the material had no significant effect on either mode frequency or mode shape in the investigation. The response of the structure corresponds with the mode shape under vibration. The shape deformation under the vibration is governed by the excitation frequency and loading conditions, including the location and the direction. Consequently, the longitudinal bending mode dominated the structural response due to the applied conditions in this investigation. Moreover, loading at the antinode vibration position provided the maximum magnitude of deformation and lower magnitude for the nodal position. Lastly, the knowledge of the structural behavior under the vibration in this study can be further used for either the effective sensor attachment or controlling the vibration in vibration-based applications.

6. ACKNOWLEDGMENT

The research on Computational Analysis of Influence Parameters on Shape Deformation of a Structure under Vibration by King Mongkut's University of Technology North Bangkok received funding support from the National Science, Research and Innovation Fund (NSRF) (KMUTNB-BasicR-64-40).

7. REFERENCES

1. Hibeller, R., *Deflections, structural analysis*. 2012, Pearson Prentice Hall, Pearson Education Inc.: Upper Saddle River, NJ, USA.
2. Hosseini, O., Malekinejad, M. and Rahgozar, R., "A closed form solution for free vibration analysis of tube-in-tube systems in tall buildings", ***International Journal of Engineering, Transactions A: Basics***, Vol. 25, No. 2, (2012), 107-114. doi: 10.5829/idosi.ije.2012.25.02a.01.
3. Serway, R.A. and Vuille, C., "College physics, Cengage Learning, (2014).
4. Liu, Y. and Chu, F., "Nonlinear vibrations of rotating thin circular cylindrical shell", ***Nonlinear Dynamics***, Vol. 67, No. 2, (2012), 1467-1479. https://doi.org/10.1007/s11071-011-0082-7
5. Baker, C., "Measurements of the natural frequencies of trees", ***Journal of Experimental Botany***, Vol. 48, No. 5, (1997), 1125-1132. https://doi.org/10.1093/jxb/48.5.1125
6. Lashin, M.M., Saleh, W.S. and Alrowais, F., "Determination of different structures' materials natural frequencies using fuzzy logic system", ***International Journal of Engineering and Advanced Technology***, Vol. 9, No. 3, (2020), 723-727. doi: 10.35940/ijeat.B3641.029320.
7. Halliday, D., Resnick, R. and Walker, J., "Fundamentals of physics, John Wiley & Sons, (2013).
8. Billah, K.Y. and Scanlan, R.H., "Resonance, tacoma narrows bridge failure, and undergraduate physics textbooks", ***American Journal of Physics***, Vol. 59, No. 2, (1991), 118-124. https://doi.org/10.1119/1.16590
9. Griggs Jr, F., "Tacoma narrows bridge failure 1940, galloping gertie part 2", ***Structure***, (2022), 60. https://www.structuremag.org/?p=19995
10. de Macêdo Wahrhaftig, A. and da Fonseca, R.M.L.R., "Representative experimental and computational analysis of the initial resonant frequency of largely deformed cantilevered beams", ***International Journal of Solids and Structures***, Vol. 102, (2016), 44-55. https://doi.org/10.1016/j.ijsolstr.2016.10.018
11. Mondal, S., Ghuku, S. and Saha, K.N., "Effect of clamping torque on large deflection static and dynamic response of a cantilever beam: An experimental study", ***International Journal of Engineering and Technologies***, Vol. 15, (2018), 1-16. https://doi.org/10.18052/www.scipress.com/IJET.15.1
12. Wahrhaftig, A., Brasil, R., Groba, T., Rocha, L., Balthazar, J. and Nascimento, L., "Resonance of a rotary machine support beam considering geometric stiffness", ***Journal of Theoretical and Applied Mechanics***, Vol. 58, (2020). doi: 10.15632/jtam-pl/126681.
13. Wahrhaftig, A.d.M., Magalhães, K.M., Silva, M.A., da Fonseca Brasil, R.M. and Banerjee, J.R., "Buckling and free vibration analysis of non-prismatic columns using optimized shape functions and rayleigh method", ***European Journal of Mechanics-A/Solids***, Vol. 94, (2022), 104543. https://doi.org/10.1016/j.euromechsol.2022.104543
14. de Macêdo Wahrhaftig, A., Dantas, J.G.L., da Fonseca Brasil, R.M.L.R. and Kloda, L., "Control of the vibration of simply supported beams using springs with proportional stiffness to the axially applied force", ***Journal of Vibration Engineering & Technologies***, (2022), 1-15. https://doi.org/10.1007/s42417-022-00502-2
15. Wahrhaftig, A.d.M., Silva, M.A.d. and Brasil, R.M., "Analytical determination of the vibration frequencies and buckling loads of slender reinforced concrete towers", ***Latin American Journal of Solids and Structures***, Vol. 16, (2019). https://doi.org/10.1590/1679-78255374
16. Wahrhaftig, A.d.M., Magalhães, K.M., Brasil, R.M. and Murawski, K., "Evaluation of mathematical solutions for the determination of buckling of columns under self-weight", ***Journal of Vibration Engineering & Technologies***, Vol. 9, No. 5, (2021), 733-749. https://doi.org/10.1007/s42417-020-00258-7
17. Ahmed, O.H., Hazem, A.-R. and Shawky, A.A., "Seismic performance of staircases in the 3d analysis of rc building", ***Civil Engineering Journal***, Vol. 7, (2022), 114-123. doi: 10.28991/CEJ-SP2021-07-08.
18. Ruiter, A.G., Veerman, J.A., Van Der Werf, K.O. and Van Hulst, N.F., "Dynamic behavior of tuning fork shear-force feedback", ***Applied Physics Letters***, Vol. 71, No. 1, (1997), 28-30. https://doi.org/10.1063/1.119482
19. Hansen, H.H., "Optimal design of an ultrasonic transducer", ***Structural Optimization***, Vol. 14, No. 2, (1997), 150-157. https://doi.org/10.1007/BF01812517
20. Gururaja, T., Schulze, W.A., Cross, L.E. and Newnham, R.E., "Piezoelectric composite materials for ultrasonic transducer applications. Part ii: Evaluation of ultrasonic medical applications", ***IEEE Transactions on Sonics and Ultrasonics***, Vol. 32, No. 4, (1985), 499-513. doi.
21. Krautkrämer, J. and Krautkrämer, H., "Ultrasonic testing of materials, Springer Science & Business Media, (2013).
22. Foorginejad, A., Taheri, M. and Mollayi, N., "A non-destructive ultrasonic testing approach for measurement and modelling of tensile strength in rubbers", ***International Journal of Engineering, Transactions C: Aspects***, Vol. 33, No. 12, (2020), 2549-2555. doi: 10.5829/IJE.2020.33.12C.16.
23. Xu, C., Xie, J., Zhang, W., Kong, Q., Chen, G. and Song, G., "Experimental investigation on the detection of multiple surface cracks using vibrothermography with a low-power piezoceramic actuator", ***Sensors***, Vol. 17, No. 12, (2017), 2705. https://doi.org/10.3390/s17122705
24. Lindgren, E., Forsyth, D., Aldrin, J. and Spencer, F., "Asm handbook, volume 17, nondestructive evaluation of materials", ***ASM International***, (2018).
25. Young, W.C., Budynas, R.G. and Sadegh, A.M., "Roark's formulas for stress and strain, McGraw-Hill Education, (2012).
26. Hassanpour, P.A., Alghemlas, K. and Betancourt, A., "Experimental modal analysis of a fixed-fixed beam under axial force", in ASME International Mechanical Engineering Congress and Exposition, American Society of Mechanical Engineers. Vol. 58370, (2017), V04AT05A053.
27. Cafeo, J.A., Trethewey, M.W. and Sommer III, H.J., "Beam element structural dynamics modification using experimental modal rotational data", (1995). doi: 10.1115/1.2874446.
28. Zhang, Z. and Zhang, C., "Mechanical properties analysis of bilayer euler-bernoulli beams based on elasticity theory", ***International Journal of Engineering, Transactions B: Applications***, Vol. 33, No. 8, (2020), 1662-1667. doi: 10.5829/ije.2020.33.08b.25.
29. Rao, S.S., "Vibration of continuous systems: John wiely & sons", ***New Jersy***, (2007).

30. Ghazwani, M.H., "Development of an analytical model for beams with two dimples in opposing directions", (2016).
31. Mehdianfar, P., Shabani, Y. and Khorshidi, K., "Natural frequency of sandwich beam structures with two dimensional functionally graded porous layers based on novel formulations", ***International Journal of Engineering, Transactions B: Applications***, Vol. 35, No. 11, (2022), 2092-2101. doi: 10.5829/IJE.2022.35.11B.04.

Persian Abstract

چکیده

درک رفتار یک سازه برای اکثر کاربردها، به ویژه تحریک در کاربردهای اولتراسونیک، ضروری است. در حال حاضر دستگاه های اولتراسونیک در زمینه های مختلف مورد استفاده قرار می گیرند و نقش اساسی در تست های غیر مخرب (NDT)دارند. رفتار ساختار باید با دستیابی به بهترین عملکرد مرتبط باشد. رفتار ارتعاشی ساختاری به فرکانس طبیعی و شکل حالت بستگی دارد. در این مطالعه سعی شده است اثر پارامترهای تاثیر بر تغییر شکل برای طراحی شرایط تحریک مناسب تعیین شود. در این مطالعه، پارامترهای تأثیر یک تیر یکنواخت، شامل هندسه، شرایط تکیه گاه و مواد، برای بررسی تأثیر آنها بر فرکانس، شکل مد و پاسخ سازه گنجانده شد. نتیجه تاثیر قابل توجه طول و شرایط تکیه گاه سازه را بر فرکانس مد، کاهش چشمگیر فرکانس مد برای نصب و پشتیبانی طولانی مدت نشان داد. این مطالعه با بررسی سه شکل حالت رایج نشان داد که شکل خمشی طولی به دلیل جهت بارگذاری غالب است. بنابراین، تغییر شکل ساختار عمدتاً توسط منبع تحریک خارجی کنترل می شود و پاسخ ساختاری بالا با اعمال تحریک در نزدیکی موقعیت آنتی گره ارتعاش دریافت می شود. با این وجود، نتیجه محاسباتی تطابق خوبی با اعتبار سنجی تحلیلی با خطای کمتر از ۱٪ نشان داد. این مطالعه منجر به درک ارتعاش می شود، که می تواند بیشتر برای اتصال موثر حسگر یا طراحی کنترل ارتعاش برنامه های اولتراسونیک مورد استفاده قرار گیرد.